

Pelargonidin-PLGA nanoparticles: Fabrication, characterization, and their effect on streptozotocin induced diabetic rats

Moumita Roy, Rajat Pal & Abhay Sankar Chakraborti*

Department of Biophysics, Molecular Biology and Bioinformatics, University of Calcutta, 92, Acharya Prafulla Chandra Road, Kolkata-700 009, West Bengal, India

Received 23 December 2015; revised 08 August 2016

Diabetes is one of the serious noncommunicable diseases affecting mankind. In India, it ranks 4th with a proportional mortality rate of 2%. Pelargonidin, a simplest anthocyanidin, is known to have potential benefit in alleviating experimental diabetes. However, insolubility in water, low stability and rapid biodegradation of pelargonidin and other flavonoids are major constraints of their effective uses. Nanocapsulation is a method of choice to overcome these limitations. We have synthesized pelargonidin-encapsulated nanoparticles by emulsion-diffusion-evaporation method using poly (D, L-lactide-co-glycolide) (PLGA), a bio-compatible polymer. The nanoparticles (P-PLGA) have been characterized by different biophysical techniques. The effects of both free pelargonidin and P-PLGA nanoparticles have been tested in streptozotocin-induced diabetic rat model. Diabetic rats were treated with 0.6 mg pelargonidin/kg body wt. or pelargonidin (P)-PLGA nanoparticles containing 0.6 mg pelargonidin/kg body wt. by intravenous injection at an interval of 3 days. Administration of two doses of P-PLGA nanoparticles proved efficient in controlling hyperglycemia and hyperlipidemia. Reduced activities of enzymatic antioxidants and elevated oxidative stress markers in diabetic rats were reverted to almost normal levels by P-PLGA nanoparticle treatment. Compared to free pelargonidin, P-PLGA nanoparticles appear to be more effective in controlling the diabetogenic effects of STZ, which may be due to improved dissolution, slow release and long-acting effect of the flavonoid in nanoparticles.

Keywords: Anthocyanidin, Diabetes mellitus, Drug delivery, Flavonoids, Hyperglycemia, Hyperlipidemia, Nanocapsulation, Oxidative stress, Poly (D, L-lactide-co-glycolide)

Diabetes mellitus (DM), a dreadful metabolic syndrome, is one of the major causes of premature illness and death worldwide. In India, it ranks 4th among noncommunicable diseases with a proportional mortality rate of 2% and a prevalence of 7.8% currently. In 2016 alone, 0.893 million people died due to DM and related complications¹. Maintaining glycemic control is the central goal of the treatment of diabetes, as hyperglycemia is primarily associated with the risk of both microvascular and macrovascular complications². Generation of oxidative and nitrosative stress mediated harmful free radicals are important aspects in diabetes pathophysiology³.

Different studies on diabetes are in progress to understand the disease mechanism more precisely, as long-term glycemic control is not often sustained by currently available antidiabetic therapeutic agents⁴. Moreover, prolonged use of them may lead to

systemic toxicity and/or drug resistance, and may cause significant diminution in glycemic responses. Even daily insulin treatment in diabetic patients sometimes may not be an ideal solution⁵. In recent years, herbal sources are being explored in search of potent new antidiabetic agents, because they are less expensive and generally have no or less side effects.

Flavonoids including anthocyanins and anthocyanidins are present in many plant based food items and beverages. Normal consumption of flavonoids, estimated to be >100 mg per day⁶, is important, as they have been shown to possess various therapeutic activities. For example, several flavonoids including quercetin^{7,8}, epicatechin⁹, rutin¹⁰, puerarin¹¹, etc., exhibit antihyperglycemic or antiglycation activities. Pelargonidin, the simplest anthocyanidin, possesses free radical scavenging ability and pharmacological activities. Findings from our as well as other laboratories have highlighted the importance of pelargonidin^{12,13} and its glycosides¹⁴ namely, pelargonidin-3-galactoside and pelargonidin-3-O-

*Correspondence:

Phone: +91 33 2350 8386 Ext. 327

E-mail: abhay_chakraborti@yahoo.co.in; ascbmbg@caluniv.ac.in

rhamnoside in alleviating hyperglycemia and oxidative stress. In a recent study, Pinna *et al.*¹⁵ have reported that proanthocyanidins from *Vitis vinifera* inhibit oxidative stress-induced vascular impairment in diabetic rats. However, therapeutic studies exploring different schedules of administration of the flavonoids are often hampered due to their extreme water insolubility, low stability and rapid biodegradation¹⁶.

In recent years, colloidal or nanoparticle technology is considered an important approach for the development of custom made drug formulations having different therapeutic modalities in various disease systems including diabetes¹⁷. The clinical benefits of nanotechnology based formulations depend on different aspects involving nature of nanoparticles, their aqueous dispersion stability, targeting capabilities and delivery of drugs¹⁸. In the preparation of drug-nanoparticle systems, carrier polymers are required for entrapment of the free drug. Poly (D,L-lactide-co-glycolide) (PLGA) has been used for developing different nanoparticle based drug delivery systems due to its good mechanical properties, low immunogenicity, low toxicity, excellent biocompatibility, and predictable biodegradation kinetics¹⁹. There has been several studies on PLGA nanoparticle based targeted delivery of gene, protein and drug molecules in different systems²⁰⁻²². PLGA has bioadhesive property and binds with mucosa of gastrointestinal tract²³. This may increase the residency time and drug absorption time from PLGA-drug formulations. The lactide/glycolide polymers are hydrolysed into natural metabolites (lactic and glycolic acids), which are easily metabolized by the citric acid cycle. Considering all these reasons, PLGA has been approved by the US FDA and European Medicine Agency in various drug delivery systems in humans¹⁹.

Pelargonidin exhibits antidiabetic activity, as shown by intraperitoneal (i.p.) administration of the flavonoid at a dose of 3 mg/kg body wt. in streptozotocin (STZ)-induced diabetic rats¹². However, therapeutic use of pelargonidin encounters two immediate problems: (i) the high dose required; and (ii) rapid degradation of the free drug. To overcome these problems, we have synthesized pelargonidin-encapsulated PLGA nanoparticles (P-PLGA nanoparticles). The nanoparticles prepared by emulsion-diffusion-evaporation method have been characterized for their size, shape, stability, entrapment efficiency etc and compared with free pelargonidin for therapeutic efficiency in the

treatment of hyperglycemia and associated complications in STZ-induced diabetic rats. P-PLGA nanoparticles enhance the therapeutic potential of the flavonoid by lowering the required dose, probably due to prevention of its degradation and slow release with longer action.

Material and Methods

Materials

Pelargonidin chloride, PLGA, Sephadex G-100, STZ, pyrogallol, bovine serum albumin (BSA), and dimethylammonium bromide (DMAB) were purchased from Sigma Chemical Company, USA. The ratio of monomers (lactic acid: glycolic acid) of PLGA polymer (MW 30,000-60,000) used in the study is 50:50. Rat insulin ELISA kit and glycohemoglobin (GHb) kit were purchased from DRG Diagnostics, Germany and Transasia Inc, India, respectively. Glucose, triglyceride and cholesterol estimation kits were obtained from Span Diagnostics, India. Other reagents were of analytical grade and purchased locally.

Preparation of pelargonidin-encapsulated PLGA (P-PLGA) nanoparticles

P-PLGA nanoparticles were prepared by conventional emulsion-diffusion-evaporation method²⁴ using DMAB as a stabilizer. Chemical structures of pelargonidin and PLGA are shown in Fig. 1A (i, ii), and a scheme for nanoparticle preparation is presented in Fig. 1A (iii). In brief, PLGA (50 mg) was dissolved in 2.5 mL ethyl acetate, to which pelargonidin (1 mg) dissolved in 500 μ L dimethyl sulfoxide (DMSO) was added with constant stirring. The organic solution was then emulsified with 5 mL distilled water containing 0.01% DMAB by stirring for 3 h. The emulsion was sonicated by a probe type sonicator for 2 min over an ice bath. The organic phase was removed by constant stirring in a water bath at 40°C. Distilled water was added to the resulting solution to make the final volume 5 mL and re-sonicated for 30 s.

Characterization of P-PLGA nanoparticles

Morphological study

The surface morphology of P-PLGA nanoparticles was determined in Transmission Electron Microscope (TEM) and Atomic Force Microscope (AFM) using Techna SE II and Nanoscope IIIA instruments, respectively. For TEM study, the samples were placed on a carbon grid and air dried for 1 min. The particles were then stained by phosphotungstic acid, dried and

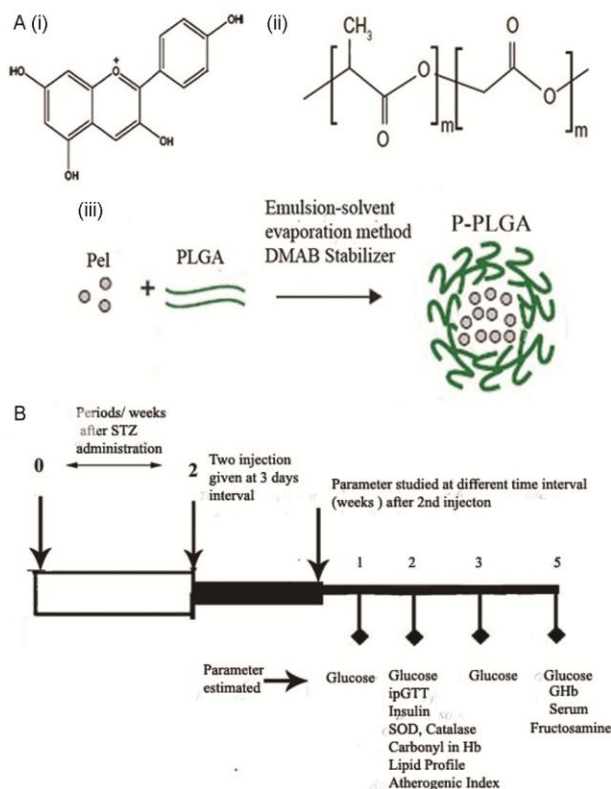


Fig. 1 — (A): (i) Pelargonidin structure, (ii) PLGA structure, and (iii) Schematic diagram for the preparation of P-PLGA nanoparticles; and (B) Schematic diagram for the experimental design of the animal experiments.

examined under TEM field. For AFM study, the samples were spread on glass slides, dried under vacuum and subjected for examination by AFM in a tapping mode.

Measurements of hydrodynamic radii, zeta potential (ζ) and polydispersity index (PDI) by dynamic light scattering (DLS)

The hydrodynamic size and PDI of P-PLGA nanoparticles were measured using a Malvern Instruments Nano ZS (Worcestershire, UK) at 25°C and the scattering angle was fixed at 175° for the measurements. ζ of P-PLGA nanoparticle suspension was measured in the same instrument. Pure water was used as a reference dispersing medium. The nanoparticle (P-PLGA) suspension used in DLS experiment contained 7.37 μ M encapsulated pelargonidin (total volume 5 mL). The experiment was done 3 times, from which the average size of P-PLGA was calculated.

Melting profile by Differential scanning calorimetry (DSC)

The thermograms of pure pelargonidin and P-PLGA nanoparticle samples were determined using DSC (DSC-7, Perkin-Elmer). The samples (1 mg each)

were heated in sealed aluminum pans at 10°C/min. The temperature was recorded from 50–400°C.

Fourier transform infrared (FTIR) study

FTIR spectra of both pelargonidin and P-PLGA nanoparticle samples on potassium bromide disks were recorded in a FTIR spectrophotometer (RX ISP-I, Perkin-Elmer). The scanning range was 400 cm^{-1} to 4000 cm^{-1} with resolution of 4 cm^{-1} .

pH Stability study

Different buffers (0.1 M acetate, 0.5 M phosphate and 0.2 M bicarbonate) having pH range from 3 to 11 were used for studying pH stability of P-PLGA nanoparticle sample. Nanoparticle suspensions (100 μ L each) were incubated with 1 mL of different buffers at 37°C for 10 min. After incubation, the tubes were centrifuged at 12000 rpm for 20 min. Pelargonidin released from P-PLGA in the supernatants was measured from absorbance at 520 nm.

Assay of pelargonidin entrapment efficiency

Encapsulation efficiency of P-PLGA was determined from the amount of pelargonidin originally taken and the amount remaining in the supernatant after harvesting the nanoparticles, as estimated by a reversed phase HPLC system (Shimadzu Corporation, Japan). Pelargonidin solution and the nanoparticle supernatants were filtered through a 0.45 μ m membrane and diluted in HPLC mobile phase (methanol). The samples (20 μ L each) were injected into the analytical column Luna (250 mm \times 4.6 mm internal diameter, particle size 5 μ m) with the flow rate (0.5 mL/min) maintained at 25°C. The wavelength of the detector was kept at 520 nm. For calibration, standard solution of pelargonidin in methanol was applied to HPLC. UV-Visible spectrophotometric method was also used for the measurement of encapsulation efficiency of pelargonidin into PLGA nanoparticles. The concentration of pelargonidin (C) used for the preparation of P-PLGA nanoparticles and its concentration remained in the supernatant (C1) after preparation of nanoparticles were measured from the respective spectrum. The encapsulation efficiency (%) of pelargonidin into PLGA nanoparticles was calculated from the relation: $(C-C1) \times 100/C$.

Animal experiments

Maintenance of animals and treatments

The study was carried out following the regulations of the Committee for the Purpose of Control and Supervision of Experiments on Animals (CPCSEA),

Government of India. The methodology was approved by the institutional Animal Ethics Committee (Registration No. 935/c/06/CPCSEA, 30.06.2009) of the University of Calcutta, Kolkata, India. Male Wistar rats, weighing 100-120 g, were obtained from University approved animal supplier, and maintained at 24-26°C, 60-80% relative humidity and on a 12 h light/dark cycle. The animals were fed a standard rat chow (Hindustan Lever, India) and had access to water *ad libitum*.

Diabetes was induced by single intraperitoneal (i.p.) injection of STZ (60 mg/kg body wt.) dissolved in 0.5 M citrate buffer, pH 4.5. Normal rats received the buffer alone. After 2 weeks of STZ administration, diabetes induction was confirmed by enhanced glucose level (≥ 200 mg/dL), as measured by using glucose estimation kit following glucose oxidase reaction in blood samples collected from tail veins. Diabetic rats were treated with P-PLGA nanoparticles or free pelargonidin solution according to the following experimental design.

Rats were divided (8 animals in each group), as follows: normal control (C), diabetic control (D), diabetic rats treated with P-PLGA (DPN), and diabetic rats treated with free pelargonidin (DP). For DPN group, diabetic rats received P-PLGA nanoparticle preparation containing 0.6 mg pelargonidin/kg body wt. by intravenous (i.v.) injection at an interval of 3 days. Two doses were administered, after which blood glucose of the treated rats dropped down to near normal level and no more dose was given. For DP group, diabetic rats were similarly treated with two doses of pelargonidin (0.6 mg/kg body wt.).

The experimental design including different parameters studied is presented in Fig. 1B. Blood samples of overnight fasting rats were collected from lateral tail veins or from the retro-orbital plexus in heparinised tubes. Blood serum was separated from the whole blood by centrifugation at $1000\times g$ for 15 min.

Estimation of glucose, glycohemoglobin (GHb), insulin and intraperitoneal glucose tolerance test (IPGTT)

Glucose was estimated in serum samples by using glucose estimation kit, as mentioned before. GHb in blood was estimated by using commercial kit containing ion-exchange resin. For estimation of insulin, blood samples were collected after 1 h of injection (i. p.) of 20% glucose solution (2 g/kg body wt.) to overnight fasting rats. Insulin was estimated in serum by using rat insulin ELISA kit following

manufacturer's protocol. For IPGTT, 20% glucose solution (2 g/kg body wt.) was injected to overnight fasting rats. Blood samples from tail vein were collected before (0 min) and 30, 60, 90 and 120 min after administration of glucose solution and used for blood glucose estimation.

Estimation of lipids

Total cholesterol (TC), total triglyceride (TG) and high density lipoprotein (HDL) in serum were estimated by using the commercially available kits. VLDL was estimated²⁵ as TG/5. LDL was calculated by using the relation²⁶: $LDL = TC - (HDL + VLDL)$, and atherogenic index (AI) was calculated from the relation²⁶: $AI = LDL/HDL$.

Estimation of antioxidant enzymes and oxidative stress markers

Superoxide dismutase (SOD) activity in serum was estimated following the method of Murklund & Murklund²⁷, based on auto-oxidation of pyrogallol. Catalase activity in serum was estimated according to the method of Aebi²⁸. Oxidative stress markers malonaldehyde (MDA) and fructosamine in serum were estimated following the methods of Yagi²⁹ and Johnson *et al.*³⁰, respectively. The protein content in serum was estimated by the method of Lowry *et al.*³¹, using BSA as the standard.

Preparation of hemoglobin (Hb) and estimation of carbonyl content

Hemolysates were prepared from red blood cells (RBC) after washing with normal saline (0.9% NaCl) and hypotonic lysis with distilled water. Hb was isolated and purified by Sephadex G-100 column chromatography, pre-equilibrated with 50 mM potassium phosphate buffer, pH 7.4. Hb concentration was measured from the Soret absorbance³², using extinction coefficient (ϵ_{415}) as $125 \text{ mM}^{-1} \text{ cm}^{-1}$ (monomer basis). Protein carbonyl content in hemoglobin was measured by using 2,4-dinitrophenyl hydrazine (2,4-DNPH), essentially following the method of Levine *et al.*³³.

Statistical analysis

Results were expressed as mean \pm SEM and statistical significance was determined by using one way analysis of variance (ANOVA). The level of significance was established at $P < 0.05$.

Results and Discussion

Characterization of P-PLGA nanoparticles

Morphology and size measurements

The shape and morphology of P-PLGA nanoparticles were determined by using TEM &

AFM. The TEM images (Fig. 2A) showed spherical nature of the particles without any aggregation or adhesion. The AFM images (Fig. 2B(i)) also showed spherical particles with smooth surface morphology. AFM 3-D image is shown in Fig. 2B(ii). The mean sizes of the particles appeared to be 91.47 ± 2.89 nm and 92.29 ± 3.04 nm, as obtained from TEM & AFM images, respectively. The histogram obtained from AFM study is shown in Fig. 2B(iii). The average diameter was calculated from a narrow range of maximum frequency of the particle sizes.

DLS experiments and entrapment efficiency studies

P-PLGA nanoparticles were characterized by DLS measurements. Representative plots of hydrodynamic Radii (Fig. 3A) and ζ (Fig. 3B) of the nanoparticles are shown. The average size, ζ and PDI of P-PLGA nanoparticles were found to be 141.8 nm, +91.9 mV and 0.148, respectively. Since DLS measurement was performed in aqueous condition, the surrounding water molecules might increase the size of the nanoparticles in comparison with those obtained by TEM and AFM methods done in dry condition. The difference in sizes obtained by microscopic and DLS methods has also been reported for quercetin-loaded PLGA and quercetin-loaded polylactic acid (PLA) nanoparticles^{34,35}. ζ Value indicates the degree of repulsion between adjacent, similarly charged particles in dispersion. For molecules and particles that are small enough, a high ζ value confers stability by resisting aggregation. Generally, ζ value of ± 30 mV is required as a minimum for a stable nanosuspension solely stabilized by electrostatic repulsion³⁶. Thus high ζ value (+91.9 mV) of P-PLGA nanoparticle suspension indicates stabilization of the formulation, which is also supported by its low PDI (0.148), suggesting monodisperse nature of the particles.

The entrapment efficiency of pelargonidin into PLGA forming P-PLGA nanoparticles was

determined by using HPLC (Fig. 3C). Free pelargonidin solution used for preparation of P-PLGA showed a peak with elution time 5.43 min (detected at 520 nm), while supernatant obtained after preparation of the nanoparticles indicated no elution of free pelargonidin. The entrapment efficiency of PLGA to form P-PLGA nanoparticles appeared to be almost 100% under our preparative condition. The entrapment efficiency was also checked by UV-Visible method. The spectra of pelargonidin solution used for the preparation of P-PLGA nanoparticles and the supernatant obtained after preparation of nanoparticles were recorded (spectra not shown). The supernatant was found to have almost no absorbance for pelargonidin, giving rise to 96.4% entrapment efficiency.

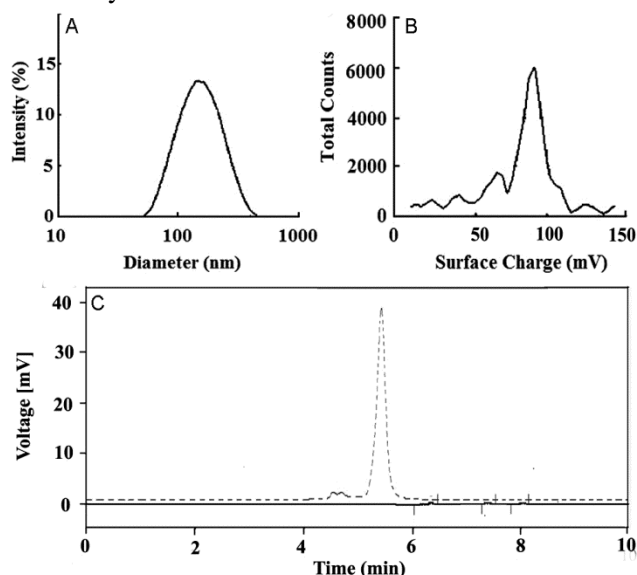


Fig. 3 — DLS experiment of P-PLGA nanoparticles. (A) Particle size distribution; (B) Surface charge (zeta potential) measurement; (C) Entrapment efficiency study: HPLC chromatograms of pelargonidin solution used for the preparation of P-PLGA nanoparticles (dotted line) and the supernatant obtained after preparation of the nanoparticles (solid line). The elution of pelargonidin was detected at 520 nm.

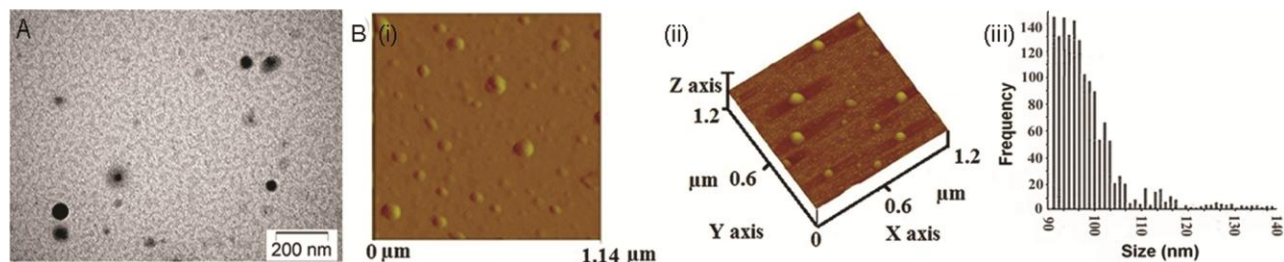


Fig. 2 — Microscopic pictures of P-PLGA nanoparticles: (A) TEM image; and (B) AFM images: (i) Surface topology, (ii) 3-D image obtained by tapping-mode and amplitude mode, respectively, and (iii) The histogram obtained from AFM study (Number of particles examined ≈ 800).

pH stability and thermal denaturation study

P-PLGA nanoparticle preparation was incubated with buffers of different pH, and pelargonidin released due to degradation of the nanoparticles was estimated (Fig. 4A). Pelargonidin release, as recorded by the absorbance at 520 nm, was the least in a buffer of pH 7, indicating maximum stability around physiological pH. The particles appeared to be quite unstable in buffers having pH less than 4 or higher than 9. Pelargonidin is quite insoluble as well as unstable in aqueous medium. Nanoencapsulation may improve solubility characteristics and enhance stability of the flavonoid in aqueous condition having normal physiological pH.

Thermal denaturation studies of pelargonidin and P-PLGA nanoparticles were done by DSC. A representative experiment is shown in Fig. 4B. The thermograms (Heat flow vs. temperature) exhibited melting temperatures (T_m) as 216.66°C for pelargonidin and 359.93°C for P-PLGA nanoparticles, depicting higher thermostable nature of the pelargonidin encoded PLGA nanoparticles. Absence of the endothermic peak of pelargonidin in the

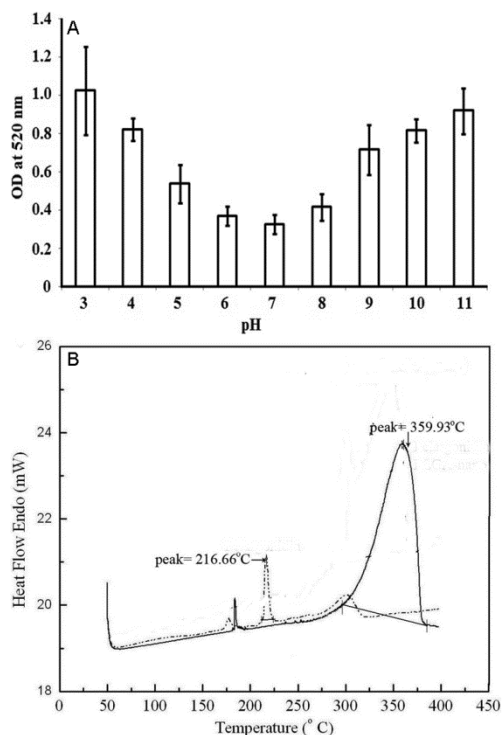


Fig. 4 — pH and thermal stability studies. (A) Amount of pelargonidin released from P-PLGA nanoparticles incubated with different buffers having pH 3-11. Results are mean \pm SE of 3 experiments; and (B) Representative DSC thermograms of pelargonidin (dotted line) and P-PLGA nanoparticles (solid line) for measurement of melting temperatures.

thermogram of P-PLGA suggests that the flavonoid is not in the crystalline form in nanoparticle formulation. However, it is dispersed throughout the polymeric capsule forming a high-energy amorphous state. P-PLGA nanoparticle, thus appears to be a new higher energy state species, and melting temperature of enclosed pelargonidin is not separately exhibited. Similar findings have also been reported by using piroxicam-polyvinylpyrrolidone nanoparticles³⁷ and quercetin-PLGA nanoparticles³⁴.

FTIR analysis

The FTIR spectrum of pelargonidin exhibited several bands characteristic of its chemical structure (Fig. 5A). Band at 3645 cm^{-1} represented $-\text{OH}$ stretch of non-bonded hydroxyl groups, whereas those present at 3303 cm^{-1} and 3182 cm^{-1} were due to the $-\text{OH}$ groups of pelargonidin. The band at 2932 cm^{-1} indicated C-H stretching of benzene ring. The bands at 1620 cm^{-1} and 1487 cm^{-1} were indicative of benzene $-\text{C}=\text{O}$ and aromatic C=C, respectively. The band at 1349 cm^{-1} was due to C-H bend. The bands present at 1160 cm^{-1} , 1079 cm^{-1} and 1023 cm^{-1} represented aromatic C-H in plane bend. Para di-substituted benzene was represented by the band at 838 cm^{-1} . The bands at 768 cm^{-1} and 694 cm^{-1} were

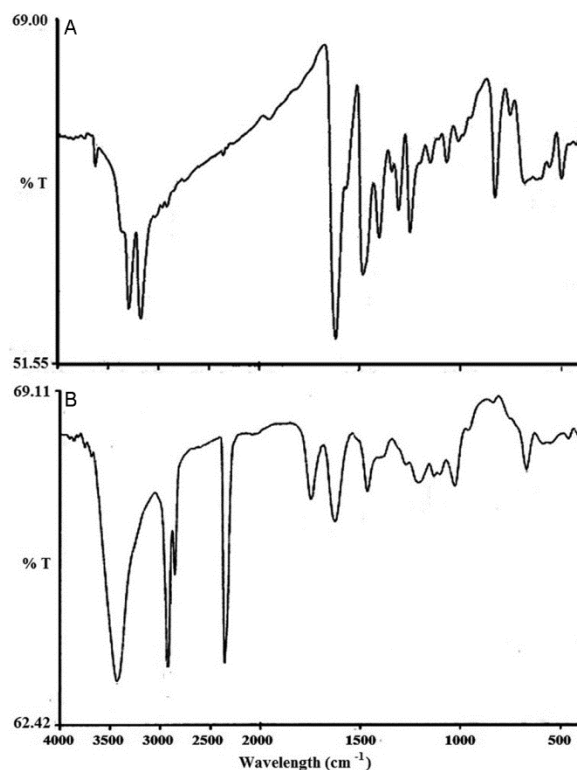


Fig. 5 — Representative FTIR spectra. (A) pelargonidin; and (B) P-PLGA nanoparticles.

due to aromatic C-H out of plane bend. As shown in the IR spectrum of P-PLGA nanoparticles (Fig. 5B), the bands responsible for the characteristic structure of pelargonidin changed and several new bands appeared like 2926 cm^{-1} and 1747 cm^{-1} , representing C-H stretch of $-\text{CH}_3$ and C=O stretch, respectively of PLGA. Instead of two sharp bands at 3303 cm^{-1} and 3182 cm^{-1} , only one broad band at 3432 cm^{-1} appeared. In IR study, P-PLGA exhibits a gross spectrum of entrapped pelargonidin and the surrounding polymeric envelope (PLGA). Similar findings including disappearance and shifting of IR bands of quercetin and catechin after encapsulation into PLGA nanoparticles have been reported^{34,38}. The changes between IR spectra of pelargonidin and P-PLGA nanoparticles as well as other characterizations confirm the entrapment of pelargonidin in PLGA nanoparticles.

Potential effect of pelargonidin as an antihyperglycemic agent is known^{12,13}. Water insolubility and quick degradation greatly restrict its ability as a good drug candidate. Compared to free pelargonidin, the therapeutic potential of P-PLGA nanoparticles has, therefore, been tested in experimental diabetes.

Animal experiments

STZ stimulates diabetes in a variety of animals by degradation of pancreatic β cells³⁹. In the present study, STZ-induced diabetes in rats was treated with both free pelargonidin and P-PLGA nanoparticles. For the treatment by both formulations, 0.6 mg pelargonidin/kg body wt. was administered at an interval of 3 days. In an earlier study, free pelargonidin (3 mg/kg body wt.) was administered (intraperitoneally) in rats to ameliorate STZ-induced diabetic complications¹². This dose showed no toxic effects in normal rats.

Glycemic status, hemoglobin glycation and insulin level in diabetes: Effect of pelargonidin and P-PLGA nanoparticles

Controlling hyperglycemia along with maintenance of stable insulin level are two most important aspects in diabetes therapy. Glucose concentration in blood serum was measured at different time intervals, as shown in Fig. 6A. STZ treatment caused a significant rise in blood glucose in group D in comparison with that in the control group C, indicating induction of diabetes in group D. After three days of administration of the 1st dose of P-PLGA nanoparticle preparation in diabetic rats (DPN), blood glucose level reduced significantly, but was still higher than

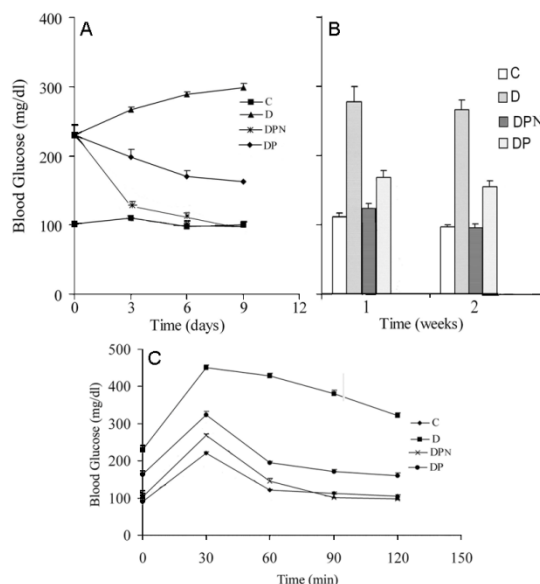


Fig. 6 — Effect of pelargonidin and P-PLGA nanoparticles on glycemic status in different groups of rat. (A) Time profile of glucose concentration (mg/dL) in blood serum of C, D, DP and DPN rats. The treatments (two doses) were made at three days interval. Results are mean \pm SE (n = 6); (B) Glucose levels in serum of different groups of rat after 1st and 2nd week from the start of the treatments. Results are mean \pm SE (n = 6); and (C) Representative curves showing glucose tolerance behavior (IPGTT). Experiments were done after two weeks of 2nd dose treatment.

the normal level. Then the 2nd dose was administered and after another three days, blood glucose level was again measured and it appeared to be almost normal in the treated group. The diabetic rats similarly treated with pelargonidin (DP) also exhibited decreased level of blood glucose. However, the treatment was less effective than P-PLGA nanoparticle treatment. Glucose levels measured in serum of different groups of rat after 1st and 2nd week from the start of the treatments together with the respective controls are shown in Fig. 6B. After normalization of blood glucose in DPN group, the level was maintained during the whole experimental period (i.e., up to 5 weeks after administration of 1st dose) (data not shown). Treatment with P-PLGA nanoparticles having 0.3 mg pelargonidin/kg body wt. was also tested, and was found to be effective with three doses (data not shown). In the present study, we used two doses of free pelargonidin and P-PLGA nanoparticle formulations having 0.6 mg pelargonidin/kg body wt.

Compared to fasting blood glucose measurement, glucose tolerance test is more reliable for recording glucose utilization. Pancreatic dysfunction leads to defective utilization of glucose by the tissues resulting

in impaired glucose tolerance and insulin imbalance. IPGTT was done in different groups of rat after two weeks of the administration of 2nd dose (Fig. 6C). Diabetic rats (D) exhibited glucose intolerant behavior in comparison with the control group (C). Glucose level in diabetic rats remained still higher after two hours of glucose load due to impaired glucose homeostasis. Blood glucose level of diabetic rats treated with P-PLGA nanoparticles (DPN) became almost normal in 120 min after glucose administration. However, in case of free pelargonidin treated group (DP), IPGTT curve was not fully normalized.

Persistent hyperglycemia results in glycation of hemoglobin, which is more or less proportional to blood glucose level. GHb level, considered as the index of diabetic condition, was measured in blood samples of different groups of rat after five weeks of the 2nd dose administration (Table 1). Compared to normal rats (C), diabetic rats (D) showed significantly elevated level of GHb, indicating poor glycemic control. The enhanced GHb level was significantly reduced by both pelargonidin (DP) and P-PLGA nanoparticle treatments (DPN). However, the levels were not fully normalized by the treatments.

Serum insulin levels were measured after two weeks of the 2nd dose treatment in DP and DPN groups and after equivalent times in C and D groups of rat. Induction of diabetes resulted in highly significant reduction in serum insulin level of group D rats compared to that of control rats (C). Free pelargonidin-treated diabetic group (DP) exhibited more or less similar insulin level as the untreated diabetic group (D). On the other hand, the level improved significantly in DPN group, indicating enhanced insulin synthesis by the nanoparticle treatment. Decrease in elevated blood glucose and normalization of glucose tolerance curve in DPN group may be due to the stimulatory activity of pelargonidin by protecting β cells of islets of

Langerhans and enhancing their functions with increased insulin level in diabetic rats. Although STZ-induced increased blood glucose level was significantly decreased by free pelargonidin (DP), there was almost no improvement of insulin level in this group. Similar result showing almost no increase in insulin level by silybin treatment in STZ-induced diabetic rats, although significant enhancement in its level by chitosan embossed silybin nanoparticles, has been reported by Das *et al.*⁴⁰. Oxidative stress condition in diabetes prevents insulin transport through endothelial walls and limits delivery of the hormone to the tissues⁴¹. Pelargonidin, being an antioxidant, may reduce oxidative stress and enhance the action of insulin resulting in decreased glucose level, although regeneration or protection of β cells is not achieved by the dose of free flavonoid used in the study. Thus formulation of nanoparticles results in improved efficacy of pelargonidin in diabetic animals. Similar approach using different nanoparticle-based delivery systems has been explored in our laboratory to enhance therapeutic potential of beneficial flavonoids, by increasing bioavailability, lowering dose requirement and reducing side effects. Antidiabetic effect of rutin is significantly enhanced using a ligand (argpyrimidine)-tagged rutin-encapsulated biocompatible (ethylene glycol dimers) nanoparticles^{42,43}. Oral delivery of quercetin⁴⁴ and naringenin⁴⁵ to diabetic rats via pH responsive alginate coated chitosan core-shell nanoparticles appears to be quite effective and may be explored as a non-invasive treatment method.

Serum lipid profiles in diabetes: Effect of pelargonidin and P-PLGA nanoparticles

Hyperglycemia and hyperlipidemia are twin co-existed problem in diabetes. Hyperlipidemia, associated with atherosclerotic disease, is a major cause of premature death in diabetes⁴⁶. Inadequate utilization of glucose in diabetes stimulates the mobilization of lipid stores, thus increasing cholesterol and triglyceride concentrations in blood⁴⁷. Serum lipid profiles were measured after two weeks of the 2nd dose in the treated (DP and DPN) and untreated control groups (C and D). In comparison with normal rats (C), diabetic rats (D) exhibited significantly higher TC level (Table 2). Both pelargonidin and P-PLGA nanoparticle treatments in diabetic rats (DP and DPN) lowered significantly the level of hypercholesterolemia. Under normal condition, insulin activates the enzyme lipoprotein

Table 1 — Effect of pelargonidin and P-PLGA treatments on GHb and serum insulin levels in diabetic rats

Parameter	C	D	DPN	DP
GHb (%)#1	4.49 ±0.56	10.52 ±1.78	7.23 ±0.46	7.97 ±0.21
Serum Insulin (mU/l) #2	44.47 ±0.012	2.02 ±0.008	15.76 ±1.13	2.07 ±0.36

[Results are mean \pm SEM of six animals of each group. #1C vs D: $P < 0.01$, D vs DPN: $P < 0.05$, D vs DP: $P < 0.05$; #2C vs D: $P < 0.01$, D vs DPN: $P < 0.01$, D vs DP: non-significant]

Table 2—Effect of pelargonidin and P-PLGA treatments on lipid profiles of diabetic rats

Parameters studied	C	D	DPN	DP
TC (mg/dL) ^{#1}	87.572 ±9.00	204.26 ±1.95	74.48 ±2.53	163.3 ±3.43
TG (mg/dL) ^{#2}	58.05 ±2.61	202.3 ±4.14	82.27 ±2.50	140.4 ±1.96
LDL (mg/dL) ^{#3}	12.79 ±1.61	140.67 ±2.52	11.08 ±1.35	100.48 ±1.03
VLDL (mg/dL) ^{#4}	11.61 ±0.52	40.46 ±0.83	16.45 ±0.50	28.08 ±0.39
HDL (mg/dL) ^{#5}	84.05 ±6.07	23.12 ±3.64	45.94 ±0.67	34.74 ±4.07
Atherogenic index ^{#6}	0.51 ±0.07	7.84 ±0.46	0.621 ±0.07	3.70 ±0.15

[Results are mean ± SEM of six animals of each group.
^{#1}C vs D: *P* <0.01, D vs DPN: *P* <0.01, D vs DP: *P* <0.05;
^{#2}C vs D: *P* <0.01, D vs DPN: *P* <0.01, D vs DP: *P* <0.01;
^{#3}C vs D: *P* <0.05, D vs DPN: *P* <0.01, D vs DP: *P* <0.01;
^{#4}C vs D: *P* <0.01, D vs DPN: *P* <0.01, D vs DP: *P* <0.05;
^{#5}C vs D: *P* <0.05, D vs DPN: *P* <0.05, D vs DP: *P* <0.05; and
^{#6}C vs D: *P* <0.01, D vs DPN: *P* <0.01, D vs DP: *P* <0.05]

lipase, which hydrolyses triglycerides. In diabetic state, lipoprotein lipase is not activated due to insulin deficiency, resulting in hypertriglyceridemia⁴⁸. TG level was found to increase significantly in diabetic rats, and the level was significantly decreased after treatment with free pelargonidin or P-PLGA nanoparticles (Table 2). Similar results were obtained with LDL and VLDL. However, all these parameters were more efficiently controlled by P-PLGA nanoparticles than free pelargonidin. Contrary to LDL, HDL exerts a role in the prevention of atherosclerosis by transporting cholesterol from peripheral tissues to liver for excretion. In comparison with control rats, HDL level decreased significantly in diabetic rats, which after treatments exhibited enhanced levels. AI, a marker of atherosclerosis, increased in diabetic rats in comparison with normal rats, and was restored to almost normal level in P-PLGA nanoparticle-treated diabetic rats (Table 2). The nanoparticle treatment thus appears to be associated with a decrease in atherosclerosis risk. Similarly, Karthick *et al.*⁴⁹ have reported the protective effect of biologically synthesized gold nanoparticles against hyperlipidemia in alloxan-induced diabetes.

Oxidative stress in diabetes: Effect of pelargonidin and P-PLGA nanoparticles

Increased generation of reactive oxygen species (ROS) and the reduced activity of antioxidant

Table 3— Effect of pelargonidin and P-PLGA treatment on enzymatic and non-enzymatic oxidative markers in diabetic rats

Parameters	C	D	DPN	DP
Serum SOD (U/mg of protein) ^{#1}	0.400 ±0.02	0.290 ±0.03	0.461 ± 0.03	0.297 ±0.07
Serum Catalase (U/mg of protein) ^{#2}	0.238 ±0.03	0.053 ±0.01	0.236 ±0.07	0.185 ±0.09
Serum Fructosamine (µmol/mg protein) ^{#3}	207 ±11.6	337 ±21.7	203 ±4.2	230 ±12.6
Carbonyl Content in Hb (µM/mg of Hb) ^{#4}	27.26 ±2.99	70.19 ±1.99	21.48 ±0.24	39.35 ±2.82

[Results are mean ± SEM of six animals of each group.
^{#1}C vs D: *P* <0.01, D vs DPN: *P* <0.01, D vs DP: non-significant;
^{#2}C vs D: *P* <0.01, D vs DPN: *P* <0.01, D vs DP: *P* <0.01;
^{#3}C vs D: *P* <0.05, D vs DPN: *P* <0.05, D vs DP: *P* <0.01; and
^{#4}C vs D: *P* <0.01, D vs DPN: *P* <0.01, D vs DP: *P* <0.05]

defenses may lead to oxidative stress in diabetic condition⁵⁰. Antioxidant enzyme activities (serum SOD and catalase) and oxidative stress markers (serum fructosamine and hemoglobin carbonyl contents) were measured in different groups of rat, as shown in Table 3. The enzyme activities and hemoglobin carbonyl content were measured two weeks after 2nd dose of treatment, while serum fructosamine level was monitored after five weeks of the treatment. Serum SOD and catalase activities were found to be significantly reduced in diabetic rats (D), as compared to those in control rats (C). The decreased enzyme activities in diabetic rats might be due to inactivation of the enzymes by ROS or by glycosylation^{51,52}. Treatment of diabetic rats with P-PLGA nanoparticles (DPN) was found to be effective in normalizing the enzyme activities. Free pelargonidin treatment (DP) caused significant increase in catalase activity, but failed to change the SOD activity.

Fructosamine is the product of protein glycation (Amadori product) at an early stage, and it undergoes oxidative cleavage resulting in the formation of advanced glycation end products (AGEs) causing diabetic complications⁵³. Serum fructosamine level appeared to be significantly higher in diabetic rats (D) than in normal rats (C). P-PLGA nanoparticle treatment normalized serum fructosamine level in diabetic rats. The treatment thus interrupts the glycation cascade, preventing the potential pathological consequences of diabetes. Free pelargonidin also exerted significant lowering effect on fructosamine level.

Carbonyl formation in proteins due to increased oxidation is another manifestation of oxidative stress⁵⁴. Such oxidatively modified proteins are

susceptible to degradation. Carbonyl contents in Hb samples isolated from treated and control groups were measured. The content appeared to be significantly higher in diabetic rats (D) than in normal rats (C). Both P-PLGA nanoparticles (DPN) and free pelargonidin (DP) treatments reversed the carbonyl stress in diabetic rats. However, DPN group exhibited more significant reversal effect, indicating effective prevention of protein modification in diabetes by pelargonidin-encoded nanoparticles. Pelargonidin-induced lowering blood glucose may inhibit glycation or carbonyl formation in the heme protein. However, Hb-flavonoid interaction, as found in a recent study⁵⁵, may also be responsible for such inhibitory effects.

Conclusion

Pelargonidin, known to reduce hyperglycemia and oxidative stress, has been successfully encapsulated by PLGA following solvent evaporation technique. The nanoparticles (P-PLGA) appear to be more effective than free pelargonidin in preventing hyperglycemia and associated pathological complications such as hyperlipidemia, cardiovascular risk and oxidative stress in experimental diabetes. Since PLGA is a safe biopolymer, the designed nanoparticle may, therefore, be used as a nanomedicine in diabetes management.

Acknowledgement

Author MR received fellowship from the University Grants Commission, New Delhi and the author RP was a research fellow under RFSMS scheme of the UGC. The work was financially supported by the Centre for Research in Nanoscience and Nanotechnology, University of Calcutta and the DST-FIST programs, Government of India, New Delhi.

Conflict of interest

The authors declare that there is no conflict of interest.

References

- 1 WHO report, World Health Organization – Diabetes country profiles, 2016. http://www.who.int/diabetes/country-profiles/ind_en.pdf?ua=1.
- 2 Michael J & Fowler MD, Microvascular and macrovascular complications of diabetes. *Clin Diabetes*, 26 (2008) 77.
- 3 Dyke KV, Jabbour N, Hoeldtke R, Dyke CV & Dyke MV, Oxidative/nitrosative stresses trigger type I diabetes: preventable in streptozotocin rats and detectable in human disease. *Ann NY Acad Sci*, 1203 (2010) 138.
- 4 Del Prato S, Felton AM, Munro N, Nesto R, Zimmet P & Zinman B, Improving glucose management: ten steps to get more patients with type 2 diabetes to glycaemic goal. *Int J Clin Pract*, 59 (2005) 1345.
- 5 Unger R & Cherrington AD, Glucagonocentric restructuring of diabetes: a pathophysiologic and therapeutic makeover. *J Clin Invest*, 122 (2012) 4.
- 6 Galvano F, Fauci LL, Lazzarino G, Fogliano V, Ritieni A, Clapellano S, Battistini NC, Tavazzi B & Galvano G, Cyanidins: metabolism and biological properties. *J Nutr Biochem*, 15 (2004) 2.
- 7 Maciel RM, Costa M, Martins DB, Franca RT, Schmatz R, Graca DL, Duarte MM, Danesi CC, Mazanti CM, Schetinger MR, Paim FC, Palma HE, Abdala FH, Stefanello N, Zimpel CK, Felin DV & Lopes ST, Antioxidant and anti-inflammatory effects of quercetin in functional and morphological alterations in streptozotocin-induced diabetic rats. *Res Vet Sci*, 95 (2013) 389.
- 8 Li JM, Wang W, Fan CY, Wang MX, Zhang X, Hu QH & Kong LD, Quercetin preserves β -cell mass and function in fructose-induced hyperinsulinemia through modulating pancreatic Akt/FoxO1 activation Evid-Based Complement. *Alternat Med*, (2013) Article ID 303902.
- 9 Fu Z, Yuskavage J & Liu D, Dietary flavonol epicatechin prevents the onset of type 1 diabetes in non obese diabetic mice. *J Agric Food Chem*, 61 (2013) 4303.
- 10 Sharma S, Ali A, Sahni JK & Baboota S, Rutin: therapeutic potential and recent advances in drug delivery, *Expert Opin Investig Drugs*, 22 (2013) 1063.
- 11 Wu K, Liang T, Duan X, Xu L, Zhang K & Li R, Anti-diabetic effects of puerarin, isolated from *Pueraria lobata* (Willd.) on streptozotocin-diabetogenic mice through promoting insulin expression and ameliorating metabolic function. *Food Chem Toxicol*, 60 (2013) 341.
- 12 Roy M, Sen S & Chakraborti AS, Action of pelargonidin on hyperglycemia and oxidative damage in diabetic rats: implication for glycation-induced hemoglobin modification. *Life Sci*, 82 (2008) 1102.
- 13 Mirshekar M, Roghani M, Khalili M, Baluchnejadmojarad T & Arab Moazzen S, Chronic oral pelargonidin alleviates streptozotocin-induced diabetic neuropathic hyperalgesia in rat: involvement of oxidative stress. *Iran Biomed J*, 14 (2010) 33.
- 14 Jayaprakasam B, Vareed SK, Olson LK & Nair MG, Insulin secretion by bioactive anthocyanins and anthocyanidins present in fruits. *J Agric Food Chem*, 53 (2005) 28.
- 15 Pinna C, Morazzoni P & Sala A, Proanthocyanidins from *Vitis vinifera* inhibit oxidative stress-induced vascular impairment in pulmonary arteries from diabetic rats. *Phytomedicine*, 25 (2017) 39.
- 16 Mohsen MAE, Marks J, Kuhnle G, Moore K, Debnam E & Srai SK, Rice-Evans C & Spencer JPE, Absorption, tissue distribution and excretion of pelargonidin and its metabolites following oral administration to rats. *Br J Nutr*, 95 (2006) 51.
- 17 Pickup JC, Zhi ZL, Khan F, Saxl T & Birch DJ, Nanomedicine and its potential in diabetes research and practice. *Diabetes Metab Res Rev*, 24 (2008) 604.
- 18 Chan VS, Nanomedicine: An unresolved regulatory issue. *Regul Toxicol Pharmacol*, 46 (2005) 218.
- 19 Danhier F, Ansorena E, Silva JM, Coco R, Le Breton A & Préat V, PLGA-based nanoparticles: an overview of biomedical applications. *J Control Release*, 161 (2012) 505.

- 20 Ramezani M, Ebrahimian M & Hashemi M, Current strategies in the modification of PLGA-based gene delivery system. *Curr Medicinal Chem*, 24 (2017) 728.
- 21 Guedj AS, Kell AJ, Barnes M, Stals S, Gonçalves D, Girard D & Lavigne C, Preparation, characterization, and safety evaluation of poly(lactide-co-glycolide) nanoparticles for protein delivery into macrophages., *Int J Nanomedicine*, 10 (2015) 5965.
- 22 Kumar R, Sahoo GC, Pandey K, Das V & Das P, Study the effects of PLGA-PEG encapsulated amphotericin B nanoparticle drug delivery system against *Leishmania donovani*. *Drug Deliv*, 22 (2015) 383.
- 23 Mahapatro A & Singh DK, Biodegradable nanoparticles are excellent vehicle for site directed in vivo delivery of drugs and vaccines. *J Nanobiotech*, 9 (2011) 55.
- 24 Hariharan S, Bhardwaj V, Bala I, Sitterberg J, Bakowasky U & Kumar MNVR, Design of estradiol loaded PLGA nanoparticulate formulations: a potential oral delivery system for hormone therapy. *Pharm Res*, 23 (2006) 184.
- 25 Friedwald WT, Levy RI & Fredrickson DS, Estimation of the concentration of LDL-cholesterol in plasma without the use of the preparative ultracentrifuge. *Clin Chem*, 18 (1972) 499.
- 26 Abbott RD, Wilson PW, Kannel WB & Castelli WP, High density lipoprotein-cholesterol, total cholesterol screening and myocardial infarction. The Framingham Study. *Arteriosclerosis*, 8 (1988) 207.
- 27 Murklund S & Murklund G, Involvement of the superoxide anion radical in the autooxidation of pyrogallol and a convenient assay for superoxide dismutase. *Eur J Biochem*, 47 (1974) 69.
- 28 Aebi H, Catalase in vivo. *Methods Enzymol*, 105 (1984) 121.
- 29 Yagi K, Lipid peroxides and human diseases. *Chem Phys Lipids*, 45 (1987) 337.
- 30 Johnson RN, Metcalf PA & Baker JR Fructosamine: a new approach to the estimation of serum glycosylation. An index of diabetic control, *Clin Chim Acta*, 127 (1982) 87.
- 31 Lowry OH, Rosebrough NJ, Farr AL & Randall RJ, Protein measurement with the Folin phenol reagent. *J Biol Chem*, 193 (1951) 265.
- 32 Bhattacharya J, Bhattacharya M, Chakraborti AS, Chaudhuri U & Poddar RK, Structural organization of hemoglobin and myoglobin influence their binding with phenothiazines. *Int J Biol Macromol*, 23 (1998) 11.
- 33 Levine RC, Garland D, Oliver CN, Amiei A, Climent I, Lanz A, Ahn B, Shalleil SO & Stadtman ER, Determination of carbonyl content in oxidatively modified proteins. *Methods Enzymol*, 186 (1990) 464.
- 34 Pal R, Roy M & Chakraborti AS, Preparation and characterization of quercetin-loaded poly (lactide-co-glycolide) nanoparticles. *Adv Sci Lett*, 10 (2012) 127.
- 35 Kumari A, Yadav SK, Pakade YB, Singh B & Yadav SC, Development of biodegradable nanoparticles for delivery of quercetin. *Colloids Surf B: Biointerfaces*, 80 (2010) 184.
- 36 Müller RH, Mäder K & Gohla S, Solid lipid nanoparticles (SLN) for controlled drug delivery - a review of the state of the art. *Eur J Pharm Biopharm*, 50 (2000) 161.
- 37 Tantishaiyakul V, Kaewnopparat N & Ingkatawornwong S, Properties of solid dispersions of piroxicaminpoly vinylpyrrolidone. *Int J Pharm*, 181 (1999) 143.
- 38 Pool H, Quintanar D, Figueroa JD, Mano CM, Bechara JEH, Godinez LA & Sandra Mendoza S, Antioxidant effects of quercetin and catechin encapsulated into PLGA nanoparticles. *J Nanomaterials*, 2012 (2012) Article ID145380.
- 39 Elsner M, Guldbakke B, Tiedge M, Munday R & Lenzen S, Relative importance of transport and alkylation for pancreatic beta-cell toxicity of streptozotocin. *Diabetologia*, 43 (2000) 1528.
- 40 Das S, Roy P, Pal R, Auddy RG, Chakraborti AS & Mukherjee A, Engineered silybin nanoparticles educe efficient control in experimental diabetes. *PLoS ONE* 9 (7) (2014) e101818.
- 41 Soto C, Mena R, Luna J, Cerbon M, Larrieta E, Vital P, Uria E, Sanchez M, Recoba R, Barron H, Farrari L & Lara A, Silymarin induces recovery of pancreatic function after alloxan damage in rats. *Life Sci*, 75 (2004) 2167.
- 42 Bhattacharjee A, Dhara K & Chakraborti AS, Argpyrimidine-tagged rutin-encapsulated biocompatible (ethylene glycol dimers) nanoparticles: Synthesis, characterization and evaluation for targeted drug delivery. *Int J Pharmaceutics*, 509 (2016) 507.
- 43 Bhattacharjee A & Chakraborti AS, Argpyrimidine-tagged rutin-encapsulated biocompatible (ethylene glycol dimers) nanoparticles: Application for targeted drug delivery in experimental diabetes (Part 2). *Int J Pharmaceutics*, 528 (2017) 8.
- 44 Mukhopadhyay P, Maity S, Chakraborty S, Rudra R, Ghodadara H, Solanki M, Chakraborti AS, Prajapati AK & Kundu PP, Oral delivery of quercetin to diabetic animals using novel pH responsive carboxypropionylated chitosan/alginate microparticles. *RSC Adv*, 6 (2016) 73210.
- 45 Maity S, Mukhopadhyay P, Kundu PP & Chakraborti AS, Alginate coated chitosan core-shell nanoparticles for efficient oral delivery of naringenin in diabetic animals - an *in vitro* and *in vivo* approach. *Carbohydr Polym*, 170 (2017) 124.
- 46 Gylling H & Miettinen TA, Cholesterol absorption, synthesis and LDL metabolism in NIDDM. *Diabetes Care*, 20 (1997) 90.
- 47 Ao Y, Chen J, Yue J & Peng RX, Effects of 18 α -glycyrrhizin on the pharmacodynamics and pharmacokinetics of glibenclamide in alloxan-induced diabetic rats. *Eur J Pharmacol*, 587 (2008) 330.
- 48 Taskinen MR, Lipoprotein lipase in diabetes. *Diabetes Metab Rev*, 2 (1987) 551.
- 49 Karthick V, Kumar VG, Dhas VG, Singaravelu G, Sadiq AM & Govindaraju K, Effect of biologically synthesized gold nanoparticles on alloxan-induced diabetic rats - an *in vivo* approach. *Colloids Surf B: Biointerfaces*, 122 (2014) 505.
- 50 Malekinejad H, Rezaabakhsh A, Rahmani F & Hobbenaghi R, Silymarin regulates the cytochrome P450 3A2 and glutathione peroxides in the liver of streptozotocin-induced diabetic rats. *Phytomedicine*, 19 (2012) 583.
- 51 Sozmen EY, Sozmen B, Delen Y & Onat T, Catalase/superoxide dismutase (SOD) and catalase/paraonase (PON) ratios may implicate poor glycemic control. *Arch Med Res*, 32 (2001) 283.

- 52 Yan H & Harding JJ, Glycation-induced inactivation and loss of antigenicity of catalase and superoxide dismutase. *Biochem J*, 328 (1997) 599.
- 53 Giardino I, Edelstein D & Brownlee M, Nonenzymatic glycosylation *in vitro* and in bovine endothelial cells alters basic fibroblast growth factor activity. A model for intracellular glycosylation in diabetes. *J Clin Invest*, 94 (1994) 110.
- 54 Donne ID, Rossi R, Giustarini D, Milzani A & Colombo R, Protein carbonyl groups as biomarkers of oxidative stress. *Clin Chim Acta*, 329 (2003) 23.
- 55 Maity S, Chakraborty S & Chakraborti AS, Critical insights into the interaction of naringenin with human haemoglobin: A combined spectroscopic and computational modeling approaches. *J Mol Struct*, 1129 (2017) 256.